Agricultural and Forest Meteorology 349 (2024) 109964

Contents lists available at ScienceDirect

Agricultural and Forest Meteorology

journal homepage: www.elsevier.com/locate/agrformet

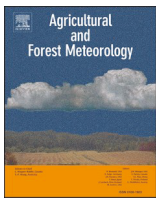

# Evaluating methods for measuring the leaf area index of encroaching shrubs in grasslands: From leaves to optical methods, 3-D scanning, and airborne observation

E. Greg Tooley [a,b,*], Jesse B. Nippert [a], Zak Ratajczak [a]

[a] Division of Biology, Kansas State University, Manhattan, KS 66506, USA
[b] Department of Biology and Graduate Degree Program in Ecology, Colorado State University, Fort Collins, CO 80523, USA

ARTICLE INFO

*Keywords:*
Leaf area index (LAI)
Ceptometer
Hyperspectral remote sensing
3D scanning
Shrub
Vertical canopy profile

ABSTRACT

Leaf area index (LAI) is a key variable describing ecosystem structure and influencing the exchange of carbon, water, and energy. LAI is often evaluated with indirect methods. However, the accuracy of indirect measurements can vary with canopy structure and is not always generalizable across ecosystems. Previous research has characterized the accuracy of indirect methods for woody plants in forest ecosystems, but it is not well established for woody plants in open ecosystems—despite having large differences in canopy structure. In this study, we compared direct LAI measurements in clonal grassland shrub canopies to three indirect methods: a ceptometer, a handheld 3D scanner (processed using EXScanPro-3.6 software), and NEON's LAI product obtained from airborne hyperspectral imaging (derived from SAVI). To our knowledge, this is the first study to assess the accuracy of leaf area data in woody plants using a handheld 3D scanner and one of few studies assessing the accuracy of the National Ecological Observation Network's (NEON) Airborne Observation Platform—our source of airborne hyperspectral imaging. Data were collected in tallgrass prairie undergoing woody encroachment and three treatments: no herbivore disturbance, bison present, and simulated browsing. We found that direct LAI measurements of control and grazed *C. drummondii* canopies averaged ~8.0. The ceptometer accurately estimated LAI in non-browsed canopies but overestimated LAI of browsed canopies by 38 %. One-sided leaf area of ramets measured with a handheld 3D scanner was strongly related to direct measurements ($r^2$=0.86), but underestimated leaf area at greater values. LAI estimated from airborne spectral data underestimated LAI by 55 %. We conclude that a ceptometer was adequate for measuring LAI in dense shrub canopies when browsing was not present, the handheld 3D scanner was adequate for measuring leaf area of individual ramets, and the airborne spectral data was not suitable for estimating LAI of dense, grassland shrub canopies.

## 1. Introduction

Leaf surfaces are the point of interaction between plants and the aboveground environment, regulating processes from carbon exchange, light extinction, and evapotranspiration to canopy interception and energy balance. The most common characterization of leaf distributions within canopies are leaf area index (LAI) and leaf area density (LAD). LAI is the total one-sided area of leaf tissue per unit ground surface area, and it represents the two-dimensional distribution of leaves in canopies (Watson, 1947). Differences in LAI are the product of changes in the density of leaves and vertical length of a canopy. LAD is the total one-sided leaf area per unit canopy volume (Weiss et al., 2004). LAD is used to characterize vertical profiles of leaf density, providing a three-dimensional perspective of leaf distributions. The ability to characterize leaf distributions has made LAI and LAD two of the most valuable and widely used measurements in the field of terrestrial ecology (Bréda, 2003).

LAI and LAD enable the integration of leaf-level process to larger scales, making them important variables in large-scale models that evaluate ecosystem structure and function, and project future climate change (Chase et al., 1996; Buermann et al., 2001; Fang et al., 2019). Most large-scale models are highly sensitive to changes in LAI (Chase et al., 1996). For example, erroneous LAI estimates from ignoring leaf clumping can cause a 13 % underestimation of global

* Corresponding author.
*E-mail address:* greg.tooley@colostate.edu (E.G. Tooley).

https://doi.org/10.1016/j.agrformet.2024.109964
Received 18 June 2023; Received in revised form 26 January 2024; Accepted 4 March 2024
Available online 12 March 2024

evapotranspiration (Chen et al., 2018). Despite this sensitivity, large-scale models rely heavily on products from airborne and space-borne observations whose accuracy is often unknown. When satellite products are evaluated, they are often compared against other indirect methods, whose measurements are also prone to inaccuracy (Yan et al., 2019), potentially leading to a propagation of errors. Understanding the accuracy of indirect methods for evaluating LAI and LAD through comparison with direct methods is critical for scaling plant and ecosystem structure and function.

Many methods exist to estimate LAI at scales ranging from leaves to landscapes (Bréda, 2003). The most accurate determination of LAI is to directly harvest leaves from sub-sections of a canopy and to individually measure leaf area using a leaf area meter or 2-D scanner (Bréda, 2003). This approach provides direct measurement of LAI but it is time-consuming and infeasible for measurements in tall canopies and at large scales. For this reason, indirect methods are commonly used to estimate LAI (Bréda, 2003). The gap fraction method uses optical sensors such as plant canopy analyzers, ceptometers, or hemispherical photography to measure LAI from light transmission (Bréda, 2003; Yan et al., 2019), based on an expanded version of Beer-Lambert law developed by Monsi and Saeki (1953):

$$I = I_o e^{(-k \times LAI)} \quad (1)$$

Where $I_o$ is the incident radiation above the canopy, $I$ is the radiation transmitted through the canopy, and $k$ is the coefficient of light extinction, which describes the rate of light extinction as light passes through foliage. $k$ is influenced by leaf arrangement, leaf angles, and solar zenith angle (Waring, 1983; Zhang et al., 2014). Plant canopy analyzers can accurately estimate LAI for most small herbaceous species (Welles and Norman, 1991; Jonckheere et al., 2004). However, optical methods assume that canopy elements are randomly dispersed and have a spherical leaf angle distribution (Campbell, 1986; Bréda, 2003; Decagon Devices, 2004; Yan et al., 2019). In larger woody species, these assumptions are rarely met (Bréda, 2003; Yan et al., 2019). Canopies with clumped or over-dispersed leaf distributions are prone to underestimation or overestimation by optical methods (Nilson, 1971; Chen, 1996; Fang et al., 2021), with LAI being underestimated by up to 70 % in clumped canopies (Chason et al., 1991; Smith et al., 1993; Stenberg, 1996; Weiss et al., 2004). The effect of leaf distribution on optical methods is quantified using a canopy clumping index (Ω), defined as a ratio of the effective LAI (LAI measured with optical methods) to the actual LAI (Nilson, 1971; Fang et al., 2021). Optical methods can also overestimate LAI when the woody proportion of the canopy increases (Chen 1996; Grower et al., 1999; Yan et al., 2019), which is typically evaluated using the canopy wood-to-total area ratio (Chen, 1996; Smolander and Stenberg, 1996; Pokorný and Marek, 2000).

Light detection and ranging (LiDAR), 3D scanners, and photogrammetry have enabled the 3D modeling of canopies to evaluate LAI and LAD (Omasa et al., 2007; Wang and Fang, 2020). To create a 3D model, scans or photographs are taken around a plant canopy and aligned to create a 3D point cloud representation of the canopy (Zheng and Moskal 2009). Point clouds are often converted to mesh models via surface reconstruction. Smoothing, hole filling, and other forms of processing can also be completed to improve the quality of the mesh model. LAI is estimated from the surface area of leaves from the model. 3D models can produce accurate LAI measurements (Thapa et al., 2018; Comba et al., 2020; Wang and Fang, 2020), but they are prone to underestimation by occlusion effects, which occur when laser or light pulses are blocked by leaves inhibiting their contact with more distant leaves (Béland et al., 2014; Soma et al., 2020; Jiang et al., 2021). Occlusion effects can be alleviated with a greater number of scanning locations and point density but become inevitable at high LAD (Soma et al., 2020; Jiang et al., 2021). Handheld 3D scanners may alleviate occlusion effects by offering a theoretically unlimited number of scan locations (Ryding et al., 2015; Bauwens et al., 2016). However, at present, the accuracy of LAI estimates from 3D handheld scanners is uncertain.

Remote sensing offers considerable promise for landscape-level ecological research, via long-term monitoring of ecological phenomena at fine to global spatial scales (Yang et al., 2013). Spectral imaging from remote sensing platforms is a common method for estimating LAI. Hyperspectral images capture information for an object across many spectral bands—often 100 s to 1000s of wavelengths of light (Adão et al., 2017; Lu et al., 2020). Previous studies have established a strong relationship between spectral reflectance and LAI, leading to the use of regression and machine learning techniques to estimate LAI from spectral bands and vegetation indices (Haboudane et al., 2004). However, we lack a single model to predict LAI based on spectral inputs (He et al., 2020), and therefore, these methods often require validation and calibration against rigorous ground-based LAI measurements (Asner et al., 2015; Pau et al., 2022). With a better understanding of the relationship between spectral reflectance and LAI across species and ecosystems at various scales, we can identify if and where approaches using hyperspectral data need improvement.

The accuracy of indirect methods for estimating LAI and LAD are well understood in forest ecosystems (Chason et al., 1991; Dufrêne and Bréda, 1995; Chen et al., 1997; Cutini et al., 1998; Pokorný and Marek, 2000), but they are not well established for woody plant canopies in open ecosystems, including grasslands, savannas, and shrublands (Ryu et al., 2010). Woody plants are common in even the most open ecosystems (Brandt et al., 2020), and they exhibit large differences in canopy structure compared to closed forests (Givnish, 1988), potentially influencing the accuracy of indirect LAI measurements. For example, leaf inclination angles vary with canopy depth in forest ecosystems but remain relatively constant for some tree species in open ecosystems (Niinemets, 1998; Ryu et al., 2010; Raabe et al., 2015; de Mattos et al., 2020). Open ecosystems also tend to be more disturbance prone than closed ecosystems causing greater variability in woody plant communities, vertical growth, and a mix of open and shade-grown growth habits (Archibald and Bond, 2003; Dantas and Pausas, 2013; Charles--Dominique et al., 2018). In ecosystems where fire is frequent, woody species often exhibit dense multilayer canopies to reduce understory biomass, facilitating fire escape (Archibald and Bond, 2003; Lett and Knapp, 2003; Brantley and Young, 2007). In ecosystems with high browsing pressure, woody plants develop high densities of branches and stems to form a protective 'cage' of woody biomass (Archibald and Bond, 2003; Staver et al., 2012; Charles-Dominique et al., 2017). These differences in canopy structure in open ecosystems are likely influencing the accuracy of indirect LAI measurements.

To evaluate the accuracy of indirect methods for estimating LAI, LAD, and leaf area in woody plant canopies of open ecosystems, this project compared three indirect methods against direct measurements in the dense, clonal canopies of *Cornus drummondii* C.A. Mey, the predominant encroaching shrub in the Kansas tallgrass prairie. To better understand the effects of grassland disturbance on the accuracy of indirect measurements, LAI comparisons were made on *C. drummondii* islands that experience three herbivory treatments: control (no herbivory), areas with bison present, and artificial removal of leaves to simulate elk herbivory (sensu Tooley et al., 2022). We included these treatments because plains bison (*Bison bison*) were the most abundant and widespread grazer and elk (*Cervus canadensis*) were the most widespread large browser in North America before European arrival. We hypothesized that: (1) ceptometer LAI measurements will underestimate direct LAI in dense *C. drummondii* canopies and become more pronounced in high LAD canopy sections. (2) A 3D handheld scanner will accurately estimate the one-sided leaf area of individual *C. drummondii* ramets when leaf area is low but deviate from this trend at larger leaf area values. (3) LAI derived from the National Ecological Observatory Network's airborne observation platform (NEON AOP) will produce poor LAI estimates for all treatments, similar to Pau et al. (2022).

## 2. Materials and methods

### 2.1. Site description

The study was conducted from mid-June through early July 2020 at the konza prairie biological station (KPBS), a 3487-ha native tallgrass prairie in the northern Flint Hills ecoregion of Kansas, USA. KPBS is divided into experimental watershed units, each with a prescribed burn treatment and grazing treatment. Both watersheds used in the study consisted of 4-year fire return intervals and have substantial encroachment by woody shrubs (*Cornus drummondii, Rhus glabra, Prunus americana*) (Ratajczak et al., 2014).

### 2.2. Experimental design

For this study, we evaluated the accuracy of indirect methods for estimating LAI in *C. drummondii* canopies across a vertical canopy profile. We also evaluated the influence of three treatments (browsing, grazing, and their absence—control). *C. drummondii* forms clonal shrub islands with dense closed canopies (see Fig. 1 for illustration). Shrub islands typically contain ~10–40 stems per square meter that expand radially using rhizomatous stems (Heisler et al., 2004; Wedel et al., 2021). Stem diameter typically varies from 3 to 50 mm basal stem diameter, with mean stem diameter of 20 mm. At maturity, islands of *C. drummondii* can exceed 10 m in diameter and have LAI values of ~8, despite having heights of only 2–4 m (Knapp et al., 2008; Ratajczak et al., 2011; Tooley et al., 2022). Fire is the main factor limiting the expansion of *C. drummondii* shrub islands (Ratajczak et al., 2014). When fire frequency is low, clonal islands expand and converge until they cover most of the landscape and leading to a closed canopy system.

Two experimental watersheds—one ungrazed (K4A) and one grazed (N4D)—were used to evaluate the effects of simulated browsing, grazing, and their absence (control) on the accuracy of LAI measurements in *C. drummondii* canopies. Both watersheds have experienced prescribed burns at a 4-year fire return interval since the 1980′s. However, watershed N4D has been continuously grazed by Great Plains bison (*Bison bison*) since 1992, while watershed K4A does not contain any large mammalian grazers. Ten distinct *C. drummondii* shrub islands were randomly selected across watershed K4A and assigned to the control and browsed treatments (5 islands/treatment), and five islands were selected across watershed N4D for the grazed treatment. *C. drummondii* islands in the control treatment ranged from 2.02 to 2.45 m in the control treatment, 1.83 to 2.47 m in the browsed treatment, and 2.03 to 2.85 m in the grazed treatment.

For islands in the browsed treatment, leaves were artificially removed to simulate elk browsing following the protocol of O'Connor et al. (2020) prior to LAI measurements (May 27th – June 1st). Fifty percent of an island's leaves along with significant amounts of new, non-woody stems were removed by hand causing occasional terminal bud damage and stem fraying. This process was done as evenly as possible throughout the entire canopy. After removal, leaves were deposited outside the study area. Islands in the grazed treatment differed

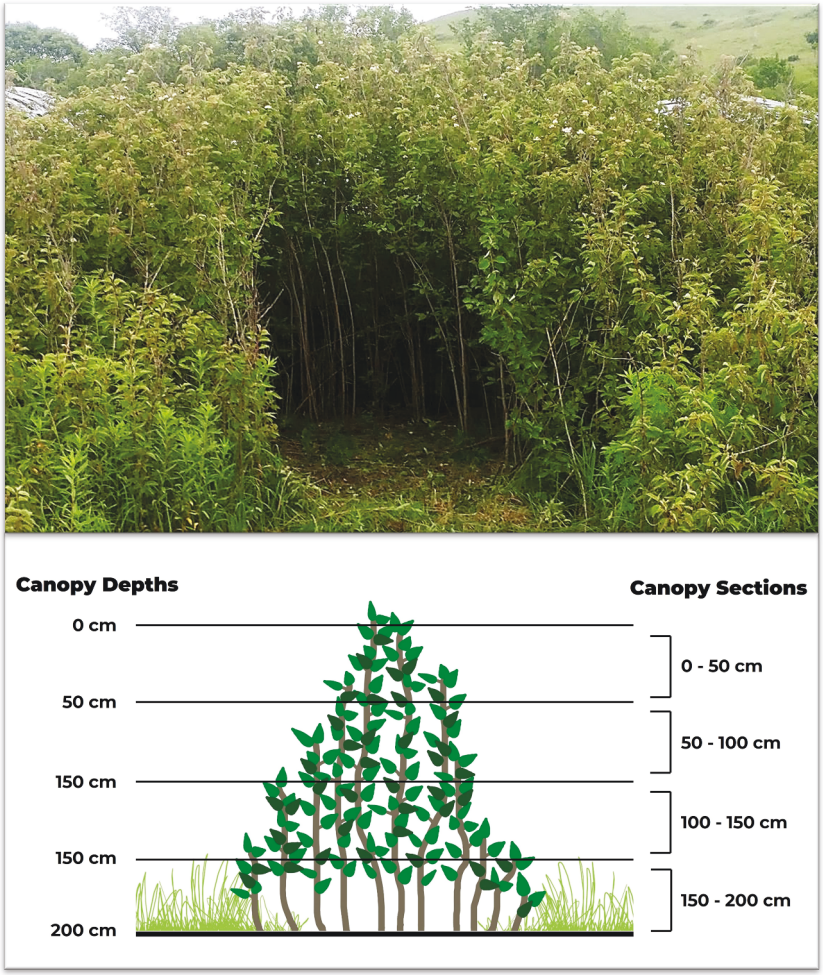


**Fig. 1.** Top: image of a *C. drummondii* shrub island with some of its interior removed to illustrate the dense canopy structure. Bottom: schematic illustrating the vertical gradient of canopy depths (0, 50, 100, 150 cm), and canopy sections (0–50, 50–100, 100–150, 150–200 cm) in *Cornus drummondii* canopies. Shrub animation by Rachel Keen with modifications.

from the browsed treatment since bison do not consume *C. drummondii* foliage. However, grazing alters fire intensity and spread, indirectly promoting woody species (Briggs et al., 2002; Van Langevelde et al., 2003; Ratajczak et al., 2014). Bison also trample stems and bed in *C. drummondii* islands, reducing woody plant abundance and resulting in a more open canopy structure (*Ratajczak et al., data*).

### 2.3. Direct measurements

To evaluate LAI, LAD, and ramet leaf area directly, a 1 $m^2$ quadrat was placed near the centers of shrub islands in the area containing the tallest ramets. All ramets in the quadrat were cut at ground level, placed in water, and transported to an indoor facility for direct measurements, which were conducted within 3 h of cutting. Before leaf removal, we performed 3-D scans of three large ramets (see below for methods). After scanning, LAI and LAD were directly measured by harvesting all leaves from the cut ramets and scanning with a LI-3100C leaf area meter (LI-COR Biosciences, Lincoln, NE USA). Leaves were harvested in 50 cm sections along a vertical canopy gradient (0–50 cm, 50–100 cm, 100–150 cm, and 150–200 cm) (Fig. 1). The height of the tallest ramet in the quadrat was considered the top of the canopy (0 cm depth). LAI was measured for each canopy section and LAD was derived from the LAI and vertical height increment of the section. Cumulative LAI was calculated for each canopy depth by adding the LAI of all sections above the given depth. We also determined the coefficient of light extinction ($k$) for canopy sections. $k$ describes the efficiency of light extinction in a canopy (Zhang et al., 2014). For each canopy section, $k$ was calculated using the directly measured LAI and the fraction of PAR interception between the top ($I_{top}$) and bottom ($I_{bottom}$) of the section. $k$ was calculated as:

$$k = -\ln\left(\frac{I_{bottom}}{I_{top}}\right) \times \frac{1}{LAI} \quad (2)$$

We also evaluated the canopy clumping index (Ω) for canopy sections by dividing the ceptometer LAI from the direct LAI.

### 2.4. Handheld 3D scanner

One-sided leaf area and leaf inclination angles ($\theta_L$) of individual *C. drummondii* ramets were evaluated using an EinScan Pro 2X Plus 3D handheld scanner. The handheld scanner collects 3D data using an LED light source. The scanner has multiple modes of scanning; handheld rapid scan was the mode used for this study. This mode has a scan accuracy of up to 0.1 mm, a frame rate of 30 frames per second, and a point distance of 0.23 – 3 mm. The scanner resolution was set to roughly 1.0 mm. This scanner is meant for scanning small to medium sized objects in an indoor environment. It has a working distance of 51 cm and a depth of field of roughly 10 cm. Thus, canopies taller than ~10 feet and those with large circumference canopies would be unfit for use with this scanner. Three large ramets from each quadrat were randomly selected for scanning. Each ramet was clipped at the base, transported indoors, and scanned to create a 3D point cloud of the ramet. Scanning was completed from all directions for roughly 10 min per ramet. EXScanPro-3.6 software was used to convert point cloud data into mesh models to evaluate one-sided leaf area and $\theta_L$. Mesh models were created using the unwater tight model option in EXScan Pro-with minimal post-processing. One-sided leaf area was calculated as half the total area of

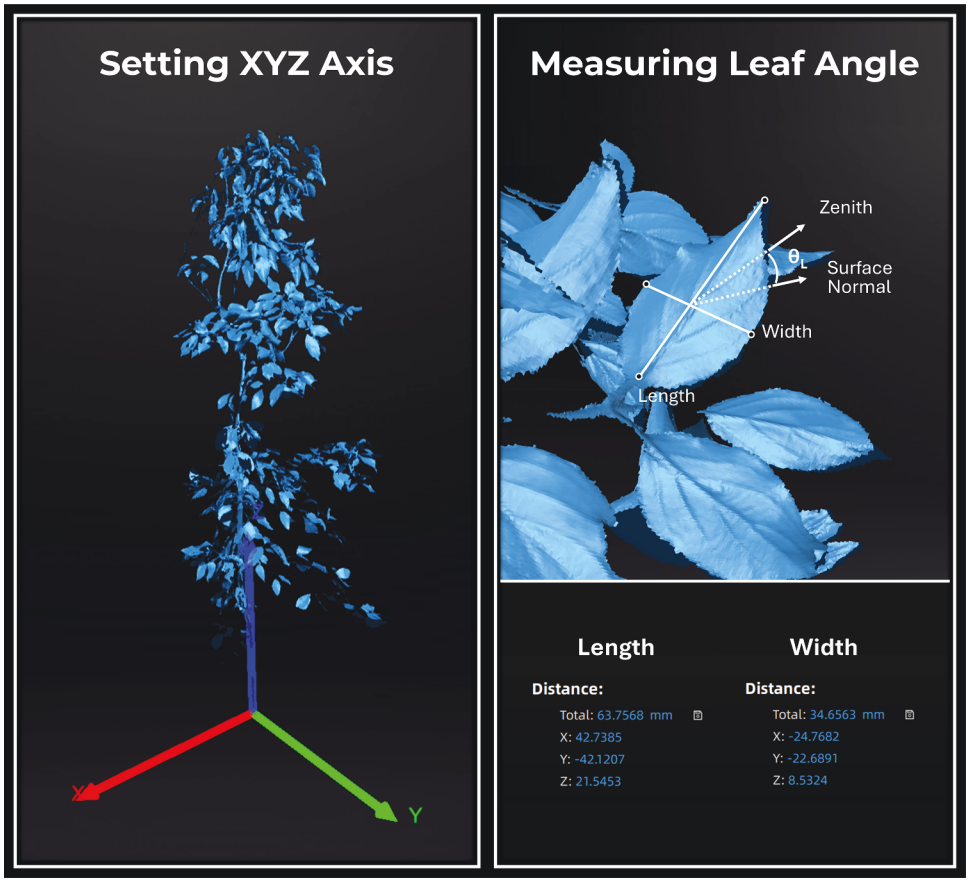


**Fig. 2.** Panels illustrating leaf inclination angle ($\theta_L$) measurements. The left panel illustrates the first step of the measurement process. Cartesian coordinates were defined for the scanned ramet, with the Z-axis (blue) representing the zenith. The right panel illustrates the $\theta_L$ measurement for an individual leaf. The leaf surface normal was derived from the cross product of two vectors spanning the length and width of the leaf. $\theta_L$ was calculated as the angle between the leaf surface normal and the zenith.

the scan, to avoid counting both tops and bottoms of leaves. Each scan consisted overwhelmingly of leaves as most branches were not readily picked up by the scanner due to their diameter and coloration (see Fig 2A for an example). $\theta_L$ was defined as the angle between the leaf surface normal and the zenith (Ross, 1981; Ryu et al., 2010), and was calculated manually using EXScanPro-3.6 software. (See Fig. 2 for method). Each leaf was treated as a flat plane. The surface normal was calculated from the cross product of two intersecting vectors spanning the length and width of the leaf (Fig. 2). $\theta_L$ was calculated as:

$$\theta_L = cos^{-1}\left(\frac{V_{Normal} \cdot V_{Zenith}}{|V_{Normal}||V_{Zenith}|}\right) \quad (3)$$

Where $V_{Normal}$ is the surface normal vector (x, y, z), $V_{Zenith}$ is the zenith vector (0, 0, 1), and the dot operator '·' represents the dot product operation. $\theta_L$ was measured at varying canopy depths for ~50 randomly selected leaves per harvested quadrat of *C. drummondii*.

### 2.5. Ceptometer LAI and light availability

Ceptometer measurements of LAI and PAR were taken over a 1 $m^2$ area near the marked, harvested area using an AccuPAR-LP-80 ceptometer. Measurements were taken in sunny conditions between the times of 12:00 and 15:00 CST across a vertical canopy gradient containing four canopy depths: 0 cm (the top of the tallest ramet), 50 cm, 100 cm, and 150 cm (Fig. 1). For each LAI measurement, eight PAR measurements were taken and averaged directly outside the canopy and at a given canopy depth. Measurements were taken from four directions (two measurements per direction; 90-degree rotation between directions). Ceptometer LAD was calculated by converting canopy depths (0, 50, 100, 150 cm) to canopy sections (0–50 cm, 50–100 cm, and 100–150 cm). The LAD of each canopy section was calculated from the difference in LAI between the top and bottom of the section.

### 2.6. NEON AOP

NEON's LAI data product (DP2.30012.001; accessed August 5th, 2022) was downloaded for July of 2020 at Konza Prairie Biological Station (NEON, 2022). The LAI product estimates the ratio of upper leaf surface area to ground area using a NEON imaging spectrometer, which is flown in flight lines at 1000 m above ground level (NEON, 2022). The timing of the fly-over is targeted for when the site is at 90 % peak greenness, which fell at the end of our sampling campaign (July 7th – 13th). The NEON imaging spectrometer (NIS) provides 420 discrete 5-nm bandpasses between 380 and 2500 nm for each pixel at a spatial resolution of 1 m (NEON, 2022). To generate reflectance data, raw NIS flight line data is processed by NEON to at-sensor radiance using NEON lab and onboard calibration information and then orthorectified using a digital surface model from co-collected lidar data. Atmospheric correction and processing of orthorectified at-sensor radiance to directional surface reflectance are completed using the modeling package ATCOR (NEON, 2022). Soil adjusted vegetation index (SAVI) is calculated from surface reflectance as the normalized ratio of 850 nm to 650 nm bands of light, after corrections applied to minimize the contribution of soil. More information about the NEON LAI product can be found on the NEON website (https://data.neonscience.org).

To estimate LAI with the NEON AOP data, the geographical coordinates were recorded for the 15 islands of *C. drummondii*. The harvested location for direct measurements was identified within each island in QGIS using NEON AOP's high-resolution orthorectified camera imagery product (NEON, 2022). The location was also confirmed through its reduced LAI value in the NEON LAI data product. The LAI of pixels surrounding the interior facing side of the harvested location were extracted and a pixel containing a near-average LAI was selected (see **Fig. S1** for LAI extraction method).

### 2.7. Statistical methods

Analysis was done in R version 4.0.2 (R Core Team, 2023). Generalized linear models were used to evaluate the response of direct cumulative LAI, direct LAD, canopy Ω, and sectional Ω to depth and treatment. A two-way ANOVA and Tukey's HSD test were performed to identify significant differences ($\alpha < 0.05$). All other relationships were evaluated with a global generalized linear model containing all predictor variables and all possible interaction terms (**Table S1; Table S2**). Transformations using log and squared terms were tested for comparisons with potential non-linear relationships. In the case of rank deficiency, multiple global models were used for separate predictor variables. For each generalized linear model, the best-fit model was selected based on the lowest AICc score and a difference of at least two units. The model selection tool 'dredge()' from the MuMIn package was used for AICc selection (Barton, 2015). For each best-fit model, an ANOVA was used to estimate the significance of model parameters, and regression analysis was performed to determine the strength of the model. For LAI comparisons between direct and indirect methods in the absence of other factors, a linear model was performed to determine the coefficient of determination ($r^2$).

## 3. Results

### 3.1. Direct measures of LAI and LAD

Direct measurements of cumulative LAI ($LAI_{direct}$) and LAD ($LAD_{direct}$) in *C. drummondii* canopies varied by treatment, depth, and their interaction (Table 1). Mean $LAI_{direct}$ was 7.6 for canopies in the control and grazed treatments and 3.2 in the browsed treatment (Fig. 3A). For all treatments, $LAD_{direct}$ of horizontal canopy sections was greatest in the 50–100 cm section compared to other canopy sections and contained nearly half of the canopies total LAI (Fig. 3b).

### 3.2. Comparison of methods

Cumulative ceptometer LAI ($LAI_{cept}$) regressed against $LAI_{direct}$ revealed a strong linear relationship with a slope of 0.89 ($r^2$=0.85; Fig. 4c). The relationship between $LAI_{cept}$ and $LAI_{direct}$ did not vary significantly by treatment and treatment was not included in the best-fit model (**Table S2, Table S3**). Despite this, the ceptometer overestimated $LAI_{direct}$ in the browsed treatment by 36 % and most values fell above the 1:1 comparison line (Fig. 4a),

The clumping index (Ω) of canopy sections varied by treatment, with a significantly greater Ω in the browsed treatment than the other

**Table 1**
ANOVA results summarizing the effects of the categorical predictor variables on the response variables. All significant effects ($P < 0.05$) are denoted with an asterisk (*). Abbreviations: LAI = leaf area index; LAD = leaf area density; $k$ = coefficient of light extinction; $\theta_L$ = leaf inclination angle; Ω = clumping index.

| Response Variable | Predictor Variable | DF | F | P |
|---|---|---|---|---|
| LAI | Depth | 4 | 69.8 | <0.001 * |
| | Treatment | 2 | 39.1 | <0.001 * |
| | Depth*Treatment | 8 | 4.39 | <0.001 * |
| LAD | Section Depth | 3 | 43.9 | <0.001 * |
| | Treatment | 2 | 17.0 | <0.001 * |
| | Section Depth*Treatment | 6 | 4.18 | 0.00185 * |
| k | Section Depth | 2 | 4.57 | 0.0175 * |
| | Treatment | 2 | 3.79 | 0.0327 * |
| | Section Depth*Treatment | 4 | 1.09 | 0.375 |
| $\theta_L$ | Section Depth | 2 | 0.21 | 0.81 |
| | Treatment | 2 | 80.0 | <0.001 * |
| | Section Depth *Treatment | 4 | 0.51 | 0.73 |
| Ω | Section Depth | 2 | 3.30 | 0.0492 * |
| | Treatment | 2 | 4.76 | 0.0151 * |
| | Section Depth*Treatment | 4 | 0.982 | 0.430 |

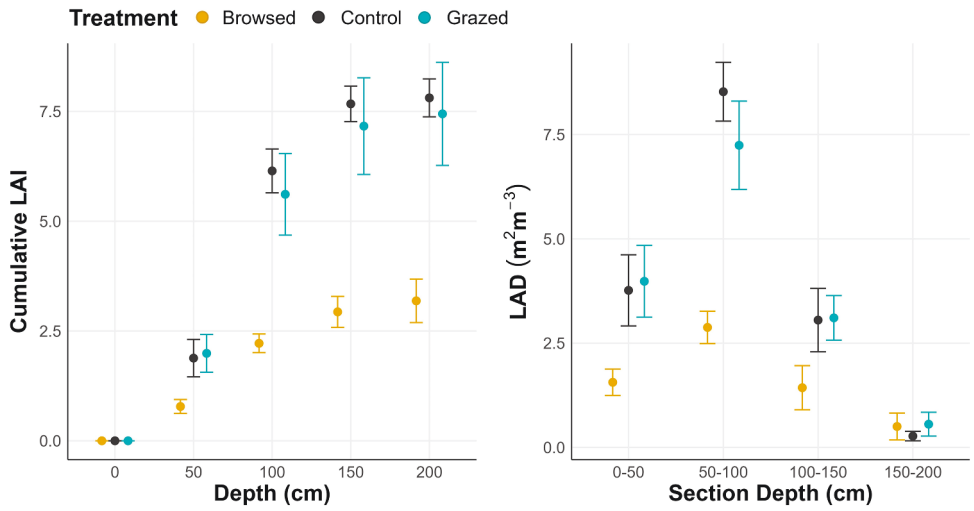


**Fig. 3.** Direct cumulative LAI measurements by canopy depth and LAD of vertical canopy sections in *C. drummondii* canopies varying by treatments (browsed, control, grazed). Point and whiskers represent the mean ± standard error.

treatments (**Fig. 5b**; Table 1). Mean Ω in the control and grazed treatments were ~1.0, while mean Ω in the browsed treatment was 1.57 (Fig. 5b). Ω of individual canopy sections also varied by depth with a greater Ω in the 0–50 cm depth compared to the other depths (Fig. 5a; Table 1).

LAD measured using a ceptometer ($LAD_{cept}$) and $LAD_{direct}$ had a significant linear relationship ($r^2$=0.52; Fig. 4d). However, the relationship between the ceptometer measurements and the direct measurements of LAD was much weaker than their relationship for measurements of LAI (Fig. 4). The best-fit model explaining $LAD_{direct}$ only included $LAD_{cept}$ (**Table S2**).

Comparison of the one-sided leaf area of individual ramets measured using the handheld 3D scanner ($LA_{3D}$) and direct measurements ($LA_{direct}$) revealed a strong linear relationship ($r^2$= 0.86). However, the slope of the linear regression model was 0.66, leading to an underestimation of $LA_{direct}$ by the 3D scanner with increasing leaf area (Fig. 4d).

LAI derived from NEON AOP ($LAI_{NEON}$) had a linear relationship with $LAI_{direct}$ ($r^2$= 0.67). However, $LAI_{NEON}$ underestimated $LAI_{direct}$ by more than 50 % and had a limited range of values compared to $LAI_{direct}$. $LAI_{NEON}$ ranged from 1.5- 3.7 while $LAI_{direct}$ ranged from 2.2- 11.0 (Fig 4e). The slope of the relationship between $LAI_{NEON}$ and $LAI_{direct}$ was 0.24, causing a greater underestimation by $LAI_{NEON}$ at higher values. This result was possibly due to $LAI_{NEON}$ values saturating around 3.5, while $LAI_{direct}$ continued to increase as one-sided leaf area increased. Similar results were found for the relationship between $LAI_{NEON}$ and $LAI_{cept}$ ($R^2$ = 0.70; Fig. 4e). $LAI_{cept}$ had a similar range of values to $LAI_{direct}$ while $LAI_{NEON}$ remained constant after reaching an LAI value of ~3.5. For comparisons between treatments, $LAI_{NEON}$ was lower in the browsed treatment compared to the control ($P < 0.001$) and grazed treatments ($P = 0.001$), a result supported by the findings from the direct method (Table 1; Fig. 3a).

### 3.3. Mechanisms

Leaf inclination angles ($\theta_L$) in *C. drummondii* canopies varied between treatments, but no differences were found by canopy depth (Table 1). Mean $\theta_L$ was similar between the browsed (53.3°) and grazed (52.6°) treatments, but more horizontally inclined in the control treatment compared to the other two treatments (33.9°; **Fig. S2**).

The coefficient of light extinction (*k*) varied by treatment and canopy depth (Table 1). *k* was greater in the browsed treatment compared to the grazed treatment, but neither treatment differed significantly from the control treatment (Fig. 6c). By canopy depth, *k* was lowest in the 0–50 cm section compared to the other sections (Fig. 6b). *k* was also affected by LAD (Table 2). LAD was included in the two best-fit models, which performed similarly at explaining differences in *k* (**Table S1**). The first model included LAD and depth ($R^2$=0.50, Table 2). This model revealed a decrease in *k* with increasing LAD for the 0–50 cm and 100–150 cm depths, but a consistently low *k* at the 50–100 cm depth. The other best-fit model only included log(LAD) ($r^2$ = 0.41; **Table S1**). In this best-fit model, *k* decreased exponentially with increasing LAD (Fig. 6a).

## 4. Discussion

The most common methods for evaluating LAI are indirect estimates, using optical instruments, LiDAR, and hyperspectral imaging (Bréda, 2003; Zheng and Moskal, 2009). However, the accuracy of indirect methods is not always evaluated, despite many of these methods, such as LiDAR, being relatively new and canopy characteristics having substantial effects on their accuracy (Chen et al., 1997; Pokorný and Marek, 2000; Bréda, 2003; Ryu et al., 2010; Fang et al., 2019). In open ecosystems including grasslands and savannas, woody plant abundance has increased rapidly in a phenomenon called "woody plant encroachment" (Archer et al., 2017; Stevens et al., 2017). Woody plants in open ecosystems exhibit large differences in canopy structure from their closed forest counterparts, potentially influencing the accuracy of indirect LAI measurements. In this study, we evaluated the accuracy of indirect methods in encroaching grassland shrub canopies, finding that: 1) an AccuPAR LP-80 ceptometer accurately estimated LAI in grazed and ungrazed watersheds but overestimated LAI by 38 % in the presence of simulated browsing. 2) An EinScan Pro 2X Plus 3D handheld scanner estimated the one-sided leaf area of individual ramets with high precision but tended to underestimate leaf area and became more biased in canopies with larger leaf areas. 3) Remotely sensed LAI estimates from NEON's airborne observatory platform were correlated with direct LAI values but underestimated LAI by 55 %.

### 4.1. Comparison of methods: ceptometer

Ceptometers and plant canopy analyzers often underestimate LAI of woody tree species (Bréda, 2003; Yan et al., 2019), with LAI estimates occasionally saturating between 5- 6 (Gower et al., 1999). However, our findings revealed that the ceptometer accurately estimated direct LAI for both control and grazed treatments. We speculate that accurate LAI estimates in our study—rather than underestimations—may be due to canopies of clonal island forming shrubs having a greater portion of woody components compared to typical tree species. While woody components were not evaluated in the current study, they are a

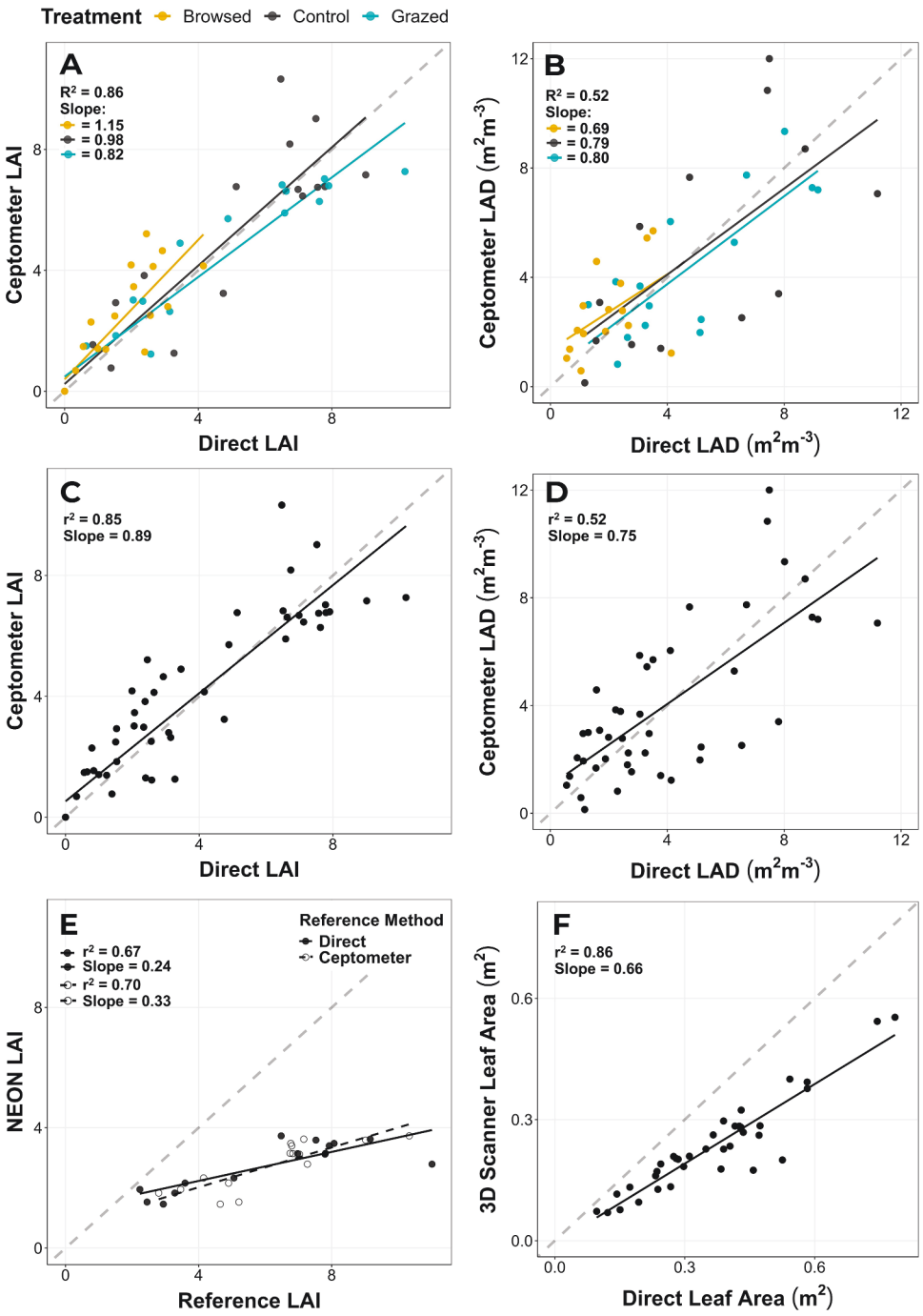


**Fig. 4.** Linear regression models of the relationships between direct and indirect measurements of the variables: (A) ceptometer LAI varying by treatment, (B) ceptometer LAD varying by treatment, (C) cemptometer LAI, (D) ceptometer LAD, (E) NEON LAI, (F) 3D scanner one-sided leaf area of individual ramets. The dashed grey line denotes a 1:1 comparison between methods.

significant factor influencing estimations of LAI in woody plant canopies (Chen, 1996; Yan et al., 2019). Previous studies have found that woody components can contribute between 3 and 40 % of the total LAI estimated for tree species by plant canopy analyzers (Gower et al., 1999; Bréda, 2003). Bréda 2003 found that the wood area index could be as high as 2.45 for *Quercus* canopies. Woody shrubs in grasslands and savannas can contain greater numbers of stems and branches compared to typical woody plants giving them a 'cage' structure to reduce herbivory (Staver et al., 2012; Charles-Dominique et al., 2017; **Fig. S3**). Extra woody surface area can potentially increase ceptometer estimates of LAI reducing their underestimation (**Fig. S3**). Alternatively, it is possible that *C. drummondii* canopy elements are more randomly dispersed (less clumped) than typical tree species. Non-random leaf dispersion (clumping) is the most common cause of underestimation in tree canopies (Nilson 1971; Chen et al., 1997; Bréda, 2003). The underestimation of LAI from clumping is typically high enough to exceed the additional LAI contributed from the woody elements of tree canopies—hence the overall underestimation by plant canopy analyzers. Therefore, an unknown is the extent to which woody components vs leaf dispersion influenced estimates of LAI by the ceptometer.

For the browsed treatment, we found that the ceptometer overestimated LAI by 38 %. Browsed canopies had a greater rate of light extinction per LAI ($k$) compared to the control and grazed treatments, despite having the most vertically inclined leaves. Increased $k$ in the

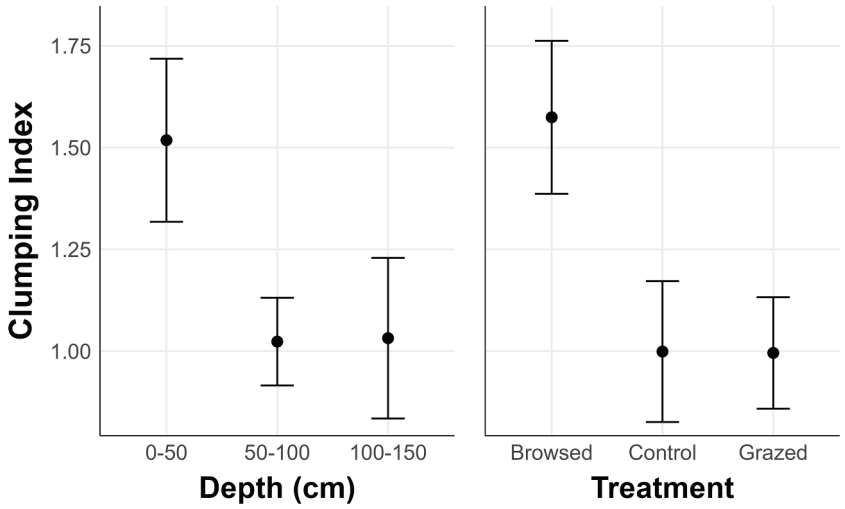


**Fig. 5.** The clumping index for *C. drummondii* canopy sections varying by depth and treatment.

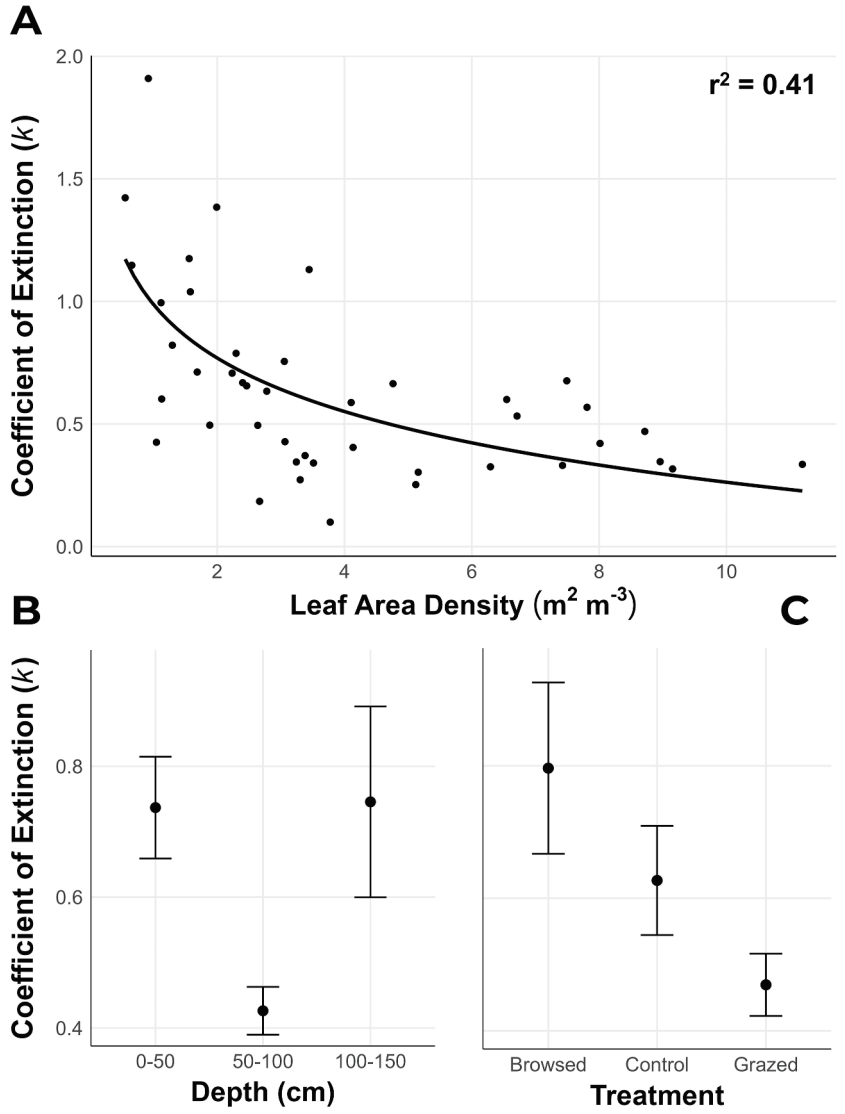


**Fig. 6.** The coefficient of light extinction (*k*) of *C. drummondii* canopy sections varying by (A) Leaf area density, (B) depth, and (C) treatment. Point and whiskers represent the mean ± standard error of measurements.

**Table 2**
ANOVA results for variables measured using direct methods in best-fit regression models. All significant effects ($P < 0.05$) are denoted with an asterisk (*). Abbreviations: $k$ = coefficient of light extinction; LAD = leaf area density.

| Variable | Model | Parameters | DF | F | P | $R^2$ |
|---|---|---|---|---|---|---|
| ***k*** | Best Fit | LAD | 1 | 19.3 | <0.001* | 0.50 |
| | | Depth | 2 | 0.61 | 0.55 | |
| | | LAD*Depth | 2 | 8.39 | <0.001* | |
| | Best Fit | log(LAD) | 1 | 27.9 | <0.001* | 0.41 |

browsed treatment was likely due to decreased leaf clumping since $k$ was greater in less dense canopy sections in all treatments. Additionally, increased $k$ and the overestimation of LAI in browsed canopies were likely the result of a greater wood to leaf ratio compared to control and grazed canopies (Chen, 1996; Yan et al., 2019), since browsed canopies had leaves removed while woody components were mostly left intact. The extent of the effect of wood to leaf ratio was not measured here, but woody components have been found to make up 21–22 % and 11 % of the total plant area index in aspen and oak-hickory forests (Chason et al., 1991; Chen et al., 1997; Gower et al., 1999), and woody-encroaching species can contain more stems and branches than forest species (Staver et al., 2012; Charles-Dominique et al., 2017). Theoretically, a reduction in leaves would influence ceptometer LAI estimates, which do not differentiate between woody and leafy canopy components.

The high sensitivity of ceptometer LAI to simulated browsing has significant implications for indirect LAI measurements in open ecosystems. Open ecosystems contain many of earth's remaining megafaunal browsers, which play a key role in shaping plant communities (Charles-Dominique et al., 2016; Malhi et al., 2016). In areas with large intact populations of megafaunal browsers, such as the African Serengeti, high intensity browsing may bias LAI estimates. In the North American Great Plains, populations of browsing herbivores including elk (*Cervus elaphus*), mule deer (*Odocoileus hemionus*), and pronghorn (*Antilocapra americana*) were largely extirpated in the late 19th century (Shaw and Lee, 1997; Rickel, 2005). Today, browser reintroductions have been proposed as a management strategy for combating woody plant encroachment (O'Connor et al., 2020; Wilcox et al., 2022). In locations where browsers have been reintroduced, approaches using ceptometers and other plant canopy analyzers will likely require site- and species-specific calibration.

### 4.2. Comparison of methods: handheld 3D scanner

Handheld 3D scanners are a promising tool for capturing complex 3D structural traits and are typically used for plant phenotyping of smaller crop species. To our knowledge, this specific technology has not been used to evaluate leaf area of woody plant canopies. The 3D handheld scanner had the best relationship with direct leaf area measurements, but it underestimated the leaf area of ramets with increasing bias at larger leaf areas. The occlusion effect likely drives this underestimation (Béland et al., 2014; Jiang et al., 2021). On multiple occurrences, we noticed that parts of leaves in the centers of larger crowns were not captured in scans. Occlusion effects are common when estimating LAI with other 3D scanning methods such as terrestrial lidar. Machine learning and automated gap filling can be used to reduce underestimation but were not used in the study. Previous research has also developed occlusion correction techniques, such as 3D kriging, to interpolate occluded areas (Soma et al., 2020). More research is needed to determine the applicability of occlusion correction techniques to handheld 3D scanners and scanners using LED instead of lidar as a source of detection. In addition to underestimation from leaf occlusion, leaf portions on the ends of branches were sometimes absent in scans due to the loss of position tracking while scanning. This often occurred on longer isolated branches and would potentially increase in species with less compact canopies. While leaf occlusion and the loss of position tracking led to some underestimation, the handheld 3D scanner had a strong relationship with direct measurements while requiring minimal post-processing ($r^2 = 0.86$). The finding indicates that 3D handheld scanners are a promising tool for evaluating leaf area of small to medium sized canopies.

### 4.3. Comparison of methods: remote sensing NEON AOP

Remote sensing could theoretically provide wall-to-wall measurements of encroachment and ensuing changes in LAI at the landscape scale. Previous studies have produced accurate LAI estimates with spectral remote sensing in some environments, including deciduous forest, shrubland, grassland, and cropland (He et al., 2020; Brantley et al., 2011; Potithep et al., 2013; Li et al., 2016; Huete, 1988; Zheng and Moskal, 2009). Our findings revealed a large, consistent, underestimation of LAI by the NEON AOP data, with most LAI estimates similar to those reported previously in the herbaceous open tallgrass prairie (Pau et al., 2022). Underestimation of LAI by the NEON LAI data increased at greater LAI. This result could indicate that the NEON LAI data is accurate but needs clumping corrected. However, underestimation of LAI may also be due to a saturation effect since NEON LAI estimates asymptote at~3.5, while direct LAI measurements continue to increase. Saturation is common for spectrometry LAI estimates in dense canopies, but typically occurs at higher values (Huete et al., 1997; Fang et al., 2019; Zhen et al., 2021). Saturation effects were found at similar LAI values (~3–4) for remotely sensed LAI estimates in canopies of *Morella cerifera*—another dense encroaching shrub (Brantley et al., 2011). Despite this, the NEON LAI data had a significant correlation with direct measurements, suggesting a potential to develop usable LAI products from this data. However, in its current state, the NEON LAI product is not suitable for 'off the shelf' usage of LAI for woody encroaching shrub canopies.

## 5. Conclusions

LAI is one of the most fundamental measurements in plant ecology. However, direct measurements of LAI consume large amounts of time and effort, which has spurred the creation of indirect methods. While many indirect methods are promising, they are often used without examining their accuracy. Comparing three very different measurements of LAI, we found that the ceptometer performed well at estimating the high LAI of *C. drummondii* shrub canopies when browsing was not present. However, the accurate LAI estimates may be due to the amount of woody stems in these canopies (**Fig. S3**). Future research is needed to better understand the accuracy of the ceptometer in dense clonal shrub canopies after accounting for woody materials. The recently developed Einscan Pro 2X Plus 3D scanner had high precision for estimating the one-sided leaf area of individual *C. drummondii* ramets but tended to underestimate at greater leaf area. The high precision and linear relationship between the 3D scanner and direct measurements makes this method suitable for estimating leaf area with the use of a simple correction factor. In contrast, airborne spectral data drastically underestimated LAI and requires further calibration to provide accurate wall-to-wall values of LAI for dense shrub canopies in grassy ecosystems.

## CRediT authorship contribution statement

**E. Greg Tooley:** Conceptualization, Data curation, Formal analysis, Investigation, Methodology, Project administration, Resources, Software, Visualization, Writing – original draft, Writing – review & editing. **Jesse B. Nippert:** Conceptualization, Funding acquisition, Investigation, Methodology, Resources, Supervision, Validation, Visualization, Writing – review & editing. **Zak Ratajczak:** Conceptualization, Investigation, Methodology, Resources, Supervision, Validation, Visualization, Writing – review & editing.

## Declaration of competing interest

The authors declare that they have no known competing financial interests or personal relationships that could have appeared to influence the work reported in this paper.

## Data availability

Data will be made available on request.

## Acknowledgements

We thank Lauren Gill, Ryan Donnelly, Emily Wedel, Rachel Keen, Seton Bachle, and the LTER research staff for assisting with data collection and browsing. Funding was provided by the Department of Energy Terrestrial Ecosystem Science Award DESC0019037, the Konza Prairie LTER program NSF DEB: 2025849, and the Kansas State University Division of Biology. Konza Prairie Biological Station provided facilities and maintenance of long-term fire and grazing treatments.

## Supplementary materials

Supplementary material associated with this article can be found, in the online version, at doi:10.1016/j.agrformet.2024.109964.

## References

Adão, T., Hruška, J., Pádua, L., Bessa, J., Peres, E., Morais, R., Sousa, J.J., 2017. Hyperspectral imaging: a review on UAV-based sensors, data processing and applications for agriculture and forestry. Remote Sens. 9 (11), 1110. https://doi.org/10.3390/rs9111110.

Archer, S.R., Andersen, E.M., Predick, K.I., Schwinning, S., Steidl, R.J., Woods, S.R., 2017. Woody plant encroachment: causes and consequences. Rangeland Systems. Springer, Cham, pp. 25–84. https://doi.org/10.1007/978-3-319-46709-2.

Archibald, S., Bond, W.J., 2003. Growing tall vs growing wide: tree architecture and allometry of Acacia karroo in forest, savanna, and arid environments. Oikos 102 (1), 3–14. https://doi.org/10.1034/j.1600-0706.2003.12181.x.

Asner, G.P., Martin, R.E., Anderson, C.B., Knapp, D.E., 2015. Quantifying forest canopy traits: imaging spectroscopy versus field survey. Remote Sens. Environ 158, 15–27. https://doi.org/10.1016/j.rse.2014.11.011.

Bréda, N.J., 2003. Ground-based measurements of leaf area index: a review of methods, instruments and current controversies. J. Exp. Bot. 54 (392), 2403–2417. https://doi.org/10.1093/jxb/erg263.

Barton, K., 2009. MuMIn: multi-model inference. R. Package. version. 1.15.1. *http://r-forge.r-project.org/projects/mumin/*.

Bauwens, S., Bartholomeus, H., Calders, K., Lejeune, P., 2016. Forest inventory with terrestrial LiDAR: a comparison of static and hand-held mobile laser scanning. Forests 7 (6), 127. https://doi.org/10.3390/f7060127.

Béland, M., Baldocchi, D.D., Widlowski, J.L., Fournier, R.A., Verstraete, M.M., 2014. On seeing the wood from the leaves and the role of voxel size in determining leaf area distribution of forests with terrestrial LiDAR. Agric. For. Meteorol 184, 82–97. https://doi.org/10.1016/j.agrformet.2013.09.005.

Brandt, M., Tucker, C.J., Kariryaa, A., Rasmussen, K., Abel, C., Small, J., Fensholt, R., 2020. An unexpectedly large count of trees in the West African Sahara and Sahel. Nature 587 (7832), 78–82. https://doi.org/10.1038/s41586-020-2824-5.

Brantley, S.T., Young, D.R., 2007. Leaf-area index and light attenuation in rapidly expanding shrub thickets. Ecology 88 (2), 524–530. https://doi.org/10.1890/06-0913.

Brantley, S.T., Zinnert, J.C., Young, D.R., 2011. Application of hyperspectral vegetation indices to detect variations in high leaf area index temperate shrub thicket canopies. Remote. Sens. Environ 115 (2), 514–523. https://doi.org/10.1016/j.rse.2010.09.020.

Briggs, J.M., Knapp, A.K., Brock, B.L., 2002. Expansion of woody plants in tallgrass prairie: a fifteen-year study of fire and fire-grazing interactions. Am. Midl. Nat. 147 (2), 287–294. https://doi.org/10.1674/0003-0031(2002)147[0287:EOWPIT]2.0.CO;2.

Buermann, W., Dong, J., Zeng, X., Myneni, R.B., Dickinson, R.E., 2001. Evaluation of the utility of satellite-based vegetation leaf area index data for climate simulations. J. Clim 14 (17), 3536–3550. https://doi.org/10.1175/1520-0442(2001)014<3536:EOTUOS>2.0.CO;2.

Campbell, G.S., 1986. Extinction coefficients for radiation in plant canopies calculated using an ellipsoidal inclination angle distribution. Agric. For. Meteorol 36 (4), 317–321. https://doi.org/10.1016/0168-1923(86)90010-9.

Charles-Dominique, T., Davies, T.J., Hempson, G.P., Bezeng, B.S., Daru, B.H., Kabongo, R.M., Bond, W.J., 2016. Spiny plants, mammal browsers, and the origin of African savannas. In: Proceedings of the National Academy of Sciences, 113, pp. E5572–E5579. https://doi.org/10.1073/pnas.160749311.

Charles-Dominique, T., Barczi, J.F., Le Roux, E., Chamaillé-Jammes, S., 2017. The architectural design of trees protects them against large herbivores. Funct. Ecol 31 (9), 1710–1717. https://doi.org/10.1111/1365-2435.12876.

Charles-Dominique, T., Midgley, G.F., Tomlinson, K.W., Bond, W.J., 2018. Steal the light: shade vs fire adapted vegetation in forest–savanna mosaics. New. Phytol 218 (4), 1419–1429. https://doi.org/10.1111/nph.15117.

Chase, T.N., Pielke, R.A., Kittel, T.G., Nemani, R., Running, S.W., 1996. Sensitivity of a general circulation model to global changes in leaf area index. Atmospheres 101 (D3), 7393–7408. https://doi.org/10.1029/95JD02417.

Chason, J.W., Baldocchi, D.D., Huston, M.A., 1991. A comparison of direct and indirect methods for estimating forest canopy leaf area. Agric. For. Meteorol 57 (1–3), 107–128. https://doi.org/10.1016/0168-1923(91)90081-Z.

Chen, J.M., 1996. Optically-based methods for measuring seasonal variation of leaf area index in boreal conifer stands. Agric. For. Meteorol 80 (2–4), 135–163. https://doi.org/10.1016/0168-1923(95)02291-0.

Chen, J.M., Rich, P.M., Gower, S.T., Norman, J.M., Plummer, S., 1997. Leaf area index of boreal forests: theory, techniques, and measurements. Atmospheres 102 (D24), 29429–29443. https://doi.org/10.1029/97JD01107.

Chen, L.H., Chen, J., Chen, C., 2018. Effect of environmental measurement uncertainty on prediction of evapotranspiration. Atmosphere 9 (10), 400. https://doi.org/10.3390/atmos9100400.

Comba, L., Biglia, A., Ricauda Aimonino, D., Tortia, C., Mania, E., Guidoni, S., Gay, P., 2020. Leaf Area Index evaluation in vineyards using 3D point clouds from UAV imagery. Prec. Agricul 21 (4), 881–896. https://doi.org/10.1007/s11119-019-09699-x.

Cutini, A., Matteucci, G., Mugnozza, G.S., 1998. Estimation of leaf area index with the Li-Cor LAI 2000 in deciduous forests. For. Ecol. Manage. 105 (1–3), 55–65. https://doi.org/10.1016/S0378-1127(97)00269-7.

Dantas, V.D.L., Pausas, J.G., 2013. The lanky and the corky: fire-escape strategies in savanna woody species. J. Ecol 101 (5), 1265–1272. https://doi.org/10.1111/1365-2745.12118.

Devices, Decagon, 2004. AccuPAR PAR/LAI ceptometer model LP-80. Oper. Manual. Version 1. 2.

de Mattos, E.M., Binkley, D., Campoe, O.C., Alvares, C.A., Stape, J.L., 2020. Variation in canopy structure, leaf area, light interception and light use efficiency among Eucalyptus clones. For. Ecol. Manage. 463, 118038 https://doi.org/10.1016/j.foreco.2020.118038.

Dufrêne, E., Bréda, N., 1995. Estimation of deciduous forest leaf area index using direct and indirect methods. Oecologia 104 (2), 156–162. https://doi.org/10.1007/BF00328580.

Fang, H., Baret, F., Plummer, S., Schaepman-Strub, G., 2019. An overview of global leaf area index (LAI): methods, products, validation, and applications. Reviews. of. Geophysics 57 (3), 739–799. https://doi.org/10.1029/2018RG000608.

Fang, H., 2021. Canopy clumping index (CI): a review of methods, characteristics, and applications. Agric. For. Meteorol 303, 108374. https://doi.org/10.1016/j.agrformet.2021.108374.

Givnish, T.J., 1988. Adaptation to sun and shade: a whole-plant perspective. Funct. Plant Biol 15 (2), 63–92. https://doi.org/10.1071/PP9880063.

Gower, S.T., Kucharik, C.J., Norman, J.M., 1999. Direct and indirect estimation of leaf area index, fAPAR, and net primary production of terrestrial ecosystems. Remote Sens. Environ 70 (1), 29–51. https://doi.org/10.1016/S0034-4257(99)00056-5.

Haboudane, D., Miller, J.R., Pattey, E., Zarco-Tejada, P.J., Strachan, I.B., 2004. Hyperspectral vegetation indices and novel algorithms for predicting green LAI of crop canopies: modeling and validation in the context of precision agriculture. Remot. Sens. Environ 90 (3), 337–352. https://doi.org/10.1016/j.rse.2003.12.013.

Heisler, J.L., Briggs, J.M., Knapp, A.K., Blair, J.M., Seery, A., 2004. Direct and indirect effects of fire on shrub density and aboveground productivity in a mesic grassland. Ecology 85 (8), 2245–2257. https://doi.org/10.1890/03-0574.

He, L., Ren, X., Wang, Y., Liu, B., Zhang, H., Liu, W., Guo, T., 2020. Comparing methods for estimating leaf area index by multi-angular remote sensing in winter wheat. Sci. Rep 10 (1), 1–11. https://doi.org/10.1038/s41598-020-70951-w.

Huete, A.R., Liu, H.Q., Batchily, K.V., Van Leeuwen, W.J.D.A., 1997. A comparison of vegetation indices over a global set of TM images for EOS-MODIS. Remote Sens. Environ 59 (3), 440–451. https://doi.org/10.1016/S0034-4257(96)00112-5.

Huete, A.R., 1988. A soil-adjusted vegetation index (SAVI). Remote Sens. Environ 25 (3), 295–309. https://doi.org/10.1016/0034-4257(88)90106-X.

Jiang, H., Hu, R., Yan, G., Cheng, S., Li, F., Qi, J., Mu, X., 2021. Influencing factors in estimation of leaf angle distribution of an individual tree from terrestrial laser scanning data. Remote Sens. 13 (6), 1159. https://doi.org/10.3390/rs13061159.

Jonckheere, I., Fleck, S., Nackaerts, K., Muys, B., Coppin, P., Weiss, M., Baret, F., 2004. Review of methods for in situ leaf area index determination: Part I. theories, sensors and hemispherical photography. Agric. For. Meteorol 121 (1–2), 19–35. https://doi.org/10.1016/j.agrformet.2003.08.027.

Knapp, A.K., Briggs, J.M., Collins, S.L., Archer, S.R., BRET-HARTE, M.S., Ewers, B.E., Cleary, M.B., 2008. Shrub encroachment in North American grasslands: shifts in growth form dominance rapidly alters control of ecosystem carbon inputs. Glob. Chang. Biol 14 (3), 615–623. https://doi.org/10.1111/j.1365-2486.2007.01512.x.

Lett, M.S., Knapp, A.K., 2003. Consequences of shrub expansion in mesic grassland: resource alterations and graminoid responses. J. Vegetation Sci 14 (4), 487–496. https://doi.org/10.1111/j.1654-1103.2003.tb02175.x.

Li, Z., Wang, J., Tang, H., Huang, C., Yang, F., Chen, B., Ge, Y., 2016. Predicting grassland leaf area index in the meadow steppes of northern china: a comparative study of regression approaches and hybrid geostatistical methods. Remote. Sens. 8 (8), 632. https://doi.org/10.3390/rs8080632.

Lu, B., Dao, P.D., Liu, J., He, Y., Shang, J., 2020. Recent advances of hyperspectral imaging technology and applications in agriculture. Remote. Sens. 12 (16), 2659. https://doi.org/10.3390/rs12162659.

Malhi, Y., Doughty, C.E., Galetti, M., Smith, F.A., Svenning, J.C., Terborgh, J.W., 2016. Megafauna and ecosystem function from the Pleistocene to the Anthropocene. In: Proceedings of the National Academy of Sciences, 113, pp. 838–846. https://doi.org/10.1073/pnas.1502540113.

NEON (National Ecological Observatory Network), January 3, 2022. LAI - spectrometer - flightline (DP2.30012.001). RELEASE-2022. https://doi.org/10.48443/n8zz-0903. Dataset accessed from. https://data.neonscience.org.on.

NEON (National Ecological Observatory Network), January 3, 2023. High-resolution orthorectified camera imagery (DP1.30010.001). RELEASE-2022. https://doi.org/10.48443/ksv5-ts70. Dataset accessed from. https://data.neonscience.org.on.

Niinemets, Ü., 1998. Adjustment of foliage structure and function to a canopy light gradient in two co-existing deciduous trees. Variability in leaf inclination angles in relation to petiole morphology. Trees 12 (7), 446–451. https://doi.org/10.1007/s004680050173.

Nilson, T., 1971. A theoretical analysis of the frequency of gaps in plant stands. Agricul. Meteorol 8, 25–38. https://doi.org/10.1016/0002-1571(71)90092-6.

O'Connor, R.C., Taylor, J.H., Nippert, J.B., 2020. Browsing and fire decreases dominance of a resprouting shrub in woody encroached grassland. Ecology 101 (2), e02935. https://doi.org/10.1002/ecy.2935.

Omasa, K., Hosoi, F., Konishi, A., 2007. 3D lidar imaging for detecting and understanding plant responses and canopy structure. J. Exp. Bot. 58 (4), 881–898. https://doi.org/10.1093/jxb/erl142.

Pau, S., Nippert, J.B., Slapikas, R., Griffith, D., Bachle, S., Helliker, B.R., Zaricor, M., 2022. Poor relationships between NEON Airborne Observation Platform data and field-based vegetation traits at a mesic grassland. Ecology 103 (2), e03590. https://doi.org/10.1002/ecy.3590.

Pokorný, R., Marek, M.V., 2000. Test of accuracy of LAI estimation by LAI-2000 under artificially changed leaf to wood area proportions. Biol. Plant. 43 (4), 537–544. https://doi.org/10.1023/A:1002862611176.

Potithep, S., Nagai, S., Nasahara, K.N., Muraoka, H., Suzuki, R., 2013. Two separate periods of the LAI–VIs relationships using in situ measurements in a deciduous broadleaf forest. Agric. For. Meteorol 169, 148–155. https://doi.org/10.1016/j.agrformet.2012.09.003.

R Core Team, 2023. R: A language and Environment for Statistical Computing. https://www.R-project.org/.

Raabe, K., Pisek, J., Sonnentag, O., Annuk, K., 2015. Variations of leaf inclination angle distribution with height over the growing season and light exposure for eight broadleaf tree species. Agric. For. Meteorol 214, 2–11. https://doi.org/10.1016/j.agrformet.2015.07.008.

Ratajczak, Z., Nippert, J.B., Hartman, J.C., Ocheltree, T.W., 2011. Positive feedbacks amplify rates of woody encroachment in mesic tallgrass prairie. Ecosphere 2 (11), 1–14. https://doi.org/10.1890/ES11-00212.1.

Ratajczak, Z., Nippert, J.B., Ocheltree, T.W., 2014a. Abrupt transition of mesic grassland to shrubland: evidence for thresholds, alternative attractors, and regime shifts. Ecology 95 (9), 2633–2645. https://doi.org/10.1890/13-1369.1.

Ratajczak, Z., Nippert, J.B., Briggs, J.M., Blair, J.M., 2014b. Fire dynamics distinguish grasslands, shrublands and woodlands as alternative attractors in the Central Great Plains of North America. Ecology 1374–1385. https://doi.org/10.1111/1365-2745.12311.

Rickel, B., 2005. Chapter 2: large native ungulates. General Technical Report RMRS-GTR-135 2. USDA Forest Service, Washington, D.C., USA, pp. 13–34.

Ross, J., 1981. The Radiation Regime and Architecture of Plant Stands. Dr W. Junk Pulishers, The Hague.

Ryding, J., Williams, E., Smith, M.J., Eichhorn, M.P., 2015. Assessing handheld mobile laser scanners for forest surveys. Remote. Sens. 7 (1), 1095–1111. https://doi.org/10.3390/rs70101095.

Ryu, Y., Sonnentag, O., Nilson, T., Vargas, R., Kobayashi, H., Wenk, R., Baldocchi, D.D., 2010. How to quantify tree leaf area index in an open savanna ecosystem: a multi-instrument and multi-model approach. Agric. For. Meteorol 150 (1), 63–76. https://doi.org/10.1016/j.agrformet.2009.08.007.

Shaw, J.H., Lee, M., 1997. Relative abundance of bison, elk, and pronghorn on the southern plains, 1806-1857. Plains Anthropol 42 (159), 163–172. https://doi.org/10.1080/2052546.1997.11931844.

Smith, N.J., Chen, J.M., Black, T.A., 1993. Effects of clumping on estimates of stand leaf area index using the LI-COR LAI-2000. Canad. J. For. Res 23 (9), 1940–1943. https://doi.org/10.1139/x93-244.

Smolander, H., Stenberg, P., 1996. Response of LAI-2000 estimates to changes in plant surface area index in a Scots pine stand. Tree Physiol. 16 (3), 345–349. https://doi.org/10.1093/treephys/16.3.345.

Soma, M., Pimont, F., Allard, D., Fournier, R., Dupuy, J.L., 2020. Mitigating occlusion effects in Leaf Area Density estimates from Terrestrial LiDAR through a specific kriging method. Remote Sens. Environ. 245, 111836 https://doi.org/10.1016/j.rse.2020.111836.

Staver, A.C., Bond, W.J., Cramer, M.D., Wakeling, J.L., 2012. Top-down determinants of niche structure and adaptation among African Acacias. Ecol. Lett. 15 (7), 673–679. https://doi.org/10.1111/j.1461-0248.2012.01784.x.

Stenberg, P., 1996. Correcting LAI-2000 estimates for the clumping of needles in shoots of conifers. Agric. For. Meteorol 79 (1–2), 1–8. https://doi.org/10.1016/0168-1923(95)02274-0.

Stevens, N., Lehmann, C.E., Murphy, B.P., Durigan, G., 2017. Savanna woody encroachment is widespread across three continents. Glob. Chang. Biol 23 (1), 235–244. https://doi.org/10.1111/gcb.13409.

Thapa, S., Zhu, F., Walia, H., Yu, H., Ge, Y., 2018. A novel LiDAR-based instrument for high-throughput, 3D measurement of morphological traits in maize and sorghum. Sensors 18 (4), 1187. https://doi.org/10.3390/s18041187.

Tooley, E.G., Nippert, J.B., Bachle, S., Keen, R.M., 2022. Intra-canopy leaf trait variation facilitates high leaf area index and compensatory growth in a clonal woody encroaching shrub. Tree Physiol. 42 (11), 2186–2202. https://doi.org/10.1093/treephys/tpac078.

Wang, Y., Fang, H., 2020. Estimation of LAI with the LiDAR technology: a review. Remote Sens. (Basel) 12 (20), 3457. https://doi.org/10.3390/rs12203457.

Waring, R.H., 1983. Estimating forest growth and efficiency in relation to canopy leaf area. In: Advances in Ecological Research, 13. Academic Press, pp. 327–354. https://doi.org/10.1016/S0065-2504(08)60111-7.

Watson, D.J., 1947. Comparative physiological studies on the growth of field crops: I. Variation in net assimilation rate and leaf area between species and varieties, and within and between years. Ann. Bot. 11 (41), 41–76.

Wedel, E.R., Nippert, J.B., Hartnett, D.C., 2021. Fire and browsing interact to alter intra-clonal stem dynamics of an encroaching shrub in tallgrass prairie. Oecologia 196 (4), 1039–1048. https://doi.org/10.1007/s00442-021-04980-1.

Weiss, M., Baret, F., Smith, G.J., Jonckheere, I., Coppin, P., 2004. Review of methods for in situ leaf area index (LAI) determination: part II. Estimation of LAI, errors and sampling. Agric. For. Meteorol 121 (1–2), 37–53. https://doi.org/10.1016/j.agrformet.2003.08.001.

Welles, J.M., Norman, J.M., 1991. Instrument for indirect measurement of canopy architecture. Agron. J 83 (5), 818–825. https://doi.org/10.2134/agronj1991.00021962008300050009x.

Wilcox, B.P., Fuhlendorf, S.D., Walker, J.W., Twidwell, D., Wu, X.B., Goodman, L.E., Birt, A., 2022. Saving imperiled grassland biomes by recoupling fire and grazing: a case study from the Great Plains. Front. Ecol. Environ 20 (3), 179–186. https://doi.org/10.1002/fee.2448.

Yan, G., Hu, R., Luo, J., Weiss, M., Jiang, H., Mu, X., Zhang, W., 2019. Review of indirect optical measurements of leaf area index: recent advances, challenges, and perspectives. Agric. For. Meteorol 265, 390–411. https://doi.org/10.1016/j.agrformet.2018.11.033.

Yang, J., Gong, P., Fu, R., Zhang, M., Chen, J., Liang, S., Dickinson, R., 2013. The role of satellite remote sensing in climate change studies. Nat. Clim. Chang 3 (10), 875–883. https://doi.org/10.1038/nclimate1908.

Zhang, L., Hu, Z., Fan, J., Zhou, D., Tang, F., 2014. A meta-analysis of the canopy light extinction coefficient in terrestrial ecosystems. Front. Earth. Sci 8 (4), 599–609. https://doi.org/10.1007/s11707-014-0446-7.

Zhen, Z., Chen, S., Yin, T., Chavanon, E., Lauret, N., Guilleux, J., Gastellu-Etchegorry, J. P., 2021. Using the negative soil adjustment factor of soil adjusted vegetation index (Savi) to resist saturation effects and estimate leaf area index (lai) in dense vegetation areas. Sensors 21 (6), 2115. https://doi.org/10.3390/s21062115.

Zheng, G., Moskal, L.M., 2009. Retrieving leaf area index (LAI) using remote sensing: theories, methods and sensors. Sensors 9 (4), 2719–2745. https://doi.org/10.3390/s90402719.